Laminar pipe flows accelerated from rest

E. A. Moss*

(Received June 1990)

An integral method was used to analyze the temporal velocity profile development in an incompressible pipe flow which has been accelerated from rest, far from end effects. As with steady state inlet flows, two fundamental zones are appropriate, corresponding to the velocity profile variation prior and subsequent to the merging of the annular boundary layer at the duct centreline, respectively. A dimensionless flow acceleration parameter (α) which arises naturally from the analysis, is zero in the case of an impulsively started flow, and possesses non-zero constant values for exponentially increasing flows. When α is increased beyond a critical value of 7.059, the boundary layer never merges. A novel flow map may be defined, containing a 'triple' point at $\alpha = 7.059$. Thus the method provides a convenient description – suitable for the application of any of the known stability analyses to unsteady pipe flows – as well as new physical insights into the basic nature of the flow field.

1. Nomenclature

d	pipe diameter	[m]
p	pressure	[Pa]
r	radial coordinate	[m]
R	pipe radius	[m]
s	velocity profile shape parameter $[= \tau_w d/(\mu U)]$	[-]
t	time	[s]
$\bar{t}$	dimensionless time $(= vt/R^2)$	[-]
u	axial velocity	[m/s]
$\bar{u}$	dimensionless axial velocity $(= u/U_c)$	[-]
U	cross-sectional mean velocity	[m/s]
U_c	dimensionless centreline $(= U_c/U)$	[-]
x	axial coordinate	[m]
y	wall coordinate	[m]
$\bar{y}$	dimensionless wall coordinate $(= y/\delta$ or $y/R)$	[-]

Greek

α	acceleration parameter $(= U^{-1}dU/dt)$	[-]
γ	pressure gradient parameter 2 $(= [R^2/U_c](\partial^2 u/\partial r^2)_0)$	[-]
δ	boundary layer thickness	[m]
δ_1	dimensionless boundary layer thickness $(= \delta/R)$	[-]
δ^*	displacement thickness	[m]
δ_1^*	dimensionless displacement thickness $(= \delta^*/R)$	[-]
λ	pressure gradient parameter 1 $(= \nu[\delta^2/U_c]dU_c/dt)$	[-]
μ	dynamic viscosity	[kg/m.s]
ν	kinematic viscosity	[m²/s]
ρ	density	[m³/s]
τ_w	wall shear stress	[N/m²]

2. Introduction

This study deals with temporally accelerating laminar flows in circular cross-section pipes. It should be viewed in the broader context of establishing an appropriate base flow model for studying the response of such flows to infinitesimal disturbances. The situation under consideration is that velocity profile development which takes place in a smooth pipe, sufficiently far from the inlet so as to exclude end effects, during the imposition of a specified flow variation with time.

Historically, Szymanski [1] was probably the first to predict analytically the development of velocity profiles in a duct subsequent to the imposition of a sudden pressure gradient. Letelier [2] measured flow rate variations with time after a step change in pressure. His results showed reasonable agreement with Szymanski's theory. Chambre et al [3] extended Szymanski's work by analyzing the flow arising from a gradually increasing pressure gradient.

Zielke [4] studied the attenuation of water hammer waves in frequency-dependent flows and in so doing derived an integral equation relating wall shear stress in transient laminar pipe flows to the instantaneous cross-sectional mean velocity and weighted past velocity changes. Indirect verification was obtained by comparison with the measured pressure fluctuations following a sudden valve closure.

More recently, Mohanty and Asthana [5] have investigated the spatial development of laminar flow in the entrance region of a smooth, uniform pipe. A fourth-degree polynomial velocity profile was used, in conjunction with the appropriately integrated conservation equations. The theoretical results obtained were verified experimentally, and were consistent with the existence of a clearly defined 'inlet' region in which a potential core was evident, as well as a 'filled' region consisting of merged velocity profiles, prior to the attainment of a parabolic velocity profile. The original identification of these fundamental flow regimes may be attributed to Ishizawa [6].

The mechanism of flow development subsequent to acceleration from rest, is diffusive. Hence, in the context of insteady flows (figure 1), the initial development zone (analogous to 'inlet' flow), prior to the merging of the boundary layers at the pipe centre, has a time-dependent potential core region adjacent to a boundary layer which thickens with time. The subsequent final development zone (analogous to the 'filled' region) is characterized by the merged boundary layers asymptotically approaching an equilibrium shape which may be parabolic.

Apparent parallels between spatial and temporal flow development indicated that an integral analysis could be applied beneficially to unsteady flows. The need for a

*Senior Lecturer
School of Mechanical Engineering
University of the Witwatersrand

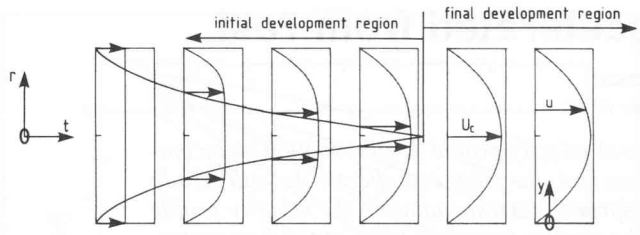

Figure 1 – Time development of velocity profiles in a pipe flow impulsively started from rest, showing the anticipated 'initial' and 'final' regions

convenient formulation of the accelerating laminar flow problem in the context of flow stability, together with the physical insight achievable by characterizing flow regimes in the manner of Mohanty and Asthana, has led to this analysis.

3. Analysis

3.1 Integral form of the governing equations

The governing conservation equations of the problem are

$$\frac{\partial u}{\partial t} = -\frac{1}{\rho}\frac{\partial p}{\partial x} + \nu\frac{1}{r}\frac{\partial}{\partial r}\left(r\frac{\partial u}{\partial r}\right) \tag{1}$$

$$\frac{\partial p}{\partial r} = 0 \tag{2}$$

where t is time, u is axial velocity, p is pressure, r is radial co-ordinate direction, x is axial co-ordinate direction, ρ is the fluid density and ν is the fluid kinematic viscosity.

These may be put into a more useful form in the following way:

At the duct centreline,

$$-\frac{1}{\rho}\frac{dp}{dx} = \frac{dU_c}{dt} - \nu\left[\frac{1}{r}\frac{\partial}{\partial r}\left(r\frac{\partial u}{\partial r}\right)\right]_0$$

where

$$\nu\left[\frac{1}{r}\frac{\partial}{\partial r}\left(r\frac{\partial u}{\partial r}\right)\right]_0 = 2\nu\left(\frac{\partial^2 u}{\partial r^2}\right)_0$$

Hence,

$$-\frac{1}{\partial}\frac{dp}{dx} = \frac{dU_c}{dt} - 2\nu\left(\frac{\partial^2 u}{\partial r^2}\right)_0$$

may be substituted into equation (1) to give

$$\frac{\partial(u - U_c)}{\partial t} = \nu\left[\frac{1}{r}\frac{\partial}{\partial r}\left(r\frac{\partial u}{\partial r}\right) - 2\left(\frac{\partial^2 u}{\partial r^2}\right)_0\right]$$

The above equation may be reduced from a (r, t) system to wall co-ordinates (y, t). The result is multiplied by $2\pi r$ and integrated across the boundary layer from $y = 0$ to $y = \delta$. Non-dimensionalisation according to $\bar{y} = y/\delta$; $\bar{u} = u/U_c$; $/\bar{t} = \nu t/R^2$; $\delta_1 = \delta/R$ and $\delta_1^* = \delta^*/R$ leads to

$$\frac{1}{U_c}\frac{d(\delta_1^* U_c)}{d\bar{t}} = \left(\frac{2}{\delta_1} - 1\right)\left(\frac{\partial^2\bar{u}}{\partial\bar{y}^2}\right)_1 + \frac{1}{\delta_1}\left(\frac{\partial\bar{u}}{\partial\bar{y}}\right)_0 \tag{3}$$

The displacement thickness in the above expression is defined by

$$\delta^* = \int_0^\delta \left(1 - \frac{u}{U_c}\right)\left(1 - \frac{y}{R}\right) dy \tag{4}$$

In addition, a mathematical statement of mass conservation for the system is

$$2\pi R U_c \delta^* \equiv \pi R^2(U_c - U) \tag{5}$$

where U is the cross-sectional mean velocity.

The final form of equations (3) and (5) will be dictated by the nature of certain dimensionless groups which emerge as a consequence of applying boundary conditions to an assumed fourth-degree polynomial velocity distribution.

3.2 Boundary conditions, polynomial velocity distribution and generalized equations.

In broad terms, if the technique of Mohanty and Asthana [5], and Ishizawa [6] is followed, two additional pressure gradient parameters λ and γ may be defined in the following way:

$$\lambda = \nu\frac{\delta^2}{U_c}\frac{dU_c}{dt}$$

$$\gamma = \frac{R^2}{U_c}\left(\frac{\partial^2 u}{\partial r^2}\right)_0$$

The dimensionless boundary conditions for the system are as follows:

(*a*) *Initial development zone*

$$\bar{u}_0 = 0$$

$$\bar{u}_1 = 1$$

$$\left(\frac{\partial\bar{u}}{\partial\bar{y}}\right)_1 = 0$$

$$\left(\frac{\partial^2\bar{u}}{\partial\bar{y}^2}\right)_1 = 0$$

$$\left(\frac{\partial^2\bar{u}}{\partial\bar{y}^2}\right)_0 - \delta_1\left(\frac{\partial\bar{u}}{\partial\bar{y}}\right)_0 = -\lambda$$

(*b*) *Final development zone*

$$\bar{u}_0 = 0$$

$$\bar{u}_1 = 1$$

$$\left(\frac{\partial\bar{u}}{\partial\bar{y}}\right)_1 = 0$$

$$\left(\frac{\partial^2\bar{u}}{\partial\bar{y}^2}\right)_1 = \gamma$$

$$\left(\frac{\partial^2\bar{u}}{\partial\bar{y}^2}\right)_0 - \left(\frac{\partial\bar{u}}{\partial\bar{y}}\right)_0 = -\gamma + 2\lambda$$

In accordance with the five boundary conditions postulated in the previous section, the following polynomial velocity distribution is assumed:

$$\bar{u} = A_0 + A_1\bar{y} + A_2\bar{y}^2 + A_3\bar{y}^3 + A_4\bar{y}^4 \quad (6)$$

where $\bar{y} = y/\delta$ and $\bar{y} = y/R$ are in the initial and final development zones, respectively.

Implementation of the boundary conditions into the assumed profile (6) yields a velocity profile of the form

$$\bar{u} = F(\bar{y}) + \lambda_1 G(\bar{y}) - \gamma_1 K(\bar{y}) \quad (7)$$

where

$$F(\bar{y}) = 2\bar{y} - 2\bar{y}^3 + \bar{y}^4$$

$$G(\bar{y}) = \frac{1}{6}(\bar{y} - 3\bar{y}^2 + 3\bar{y}^3 - \bar{y}^4)$$

$$K(\bar{y}) = \bar{y} - \frac{13}{2}\bar{y}^2 + 10\bar{y}^3 - \frac{9}{2}\bar{y}^4$$

$$\lambda_1 = 6\frac{\lambda - 2\delta_1}{6 + \delta_1}$$

$$\gamma_1 = \frac{\gamma}{6 + \delta_1}$$

$$\delta_1 = \frac{\delta}{R}$$

If $\delta_1 = 1$ in the final zone, its end is defined by $\lambda_1 = -12/7$ together with $\gamma_1 = -2/7$, thus indicating an asymptotic tendency towards a parabolic velocity profile of the form

$$\bar{u} = 2\bar{y} - \bar{y}^2$$

This describes steady state Hagen-Poiseuille flow.

Substitution of the polynomial expression (6) into equation (4) leads to the following dimensionless expression for the displacement thickness:

$$\frac{\delta^*}{R} = \delta_1^* = \delta_1\left(\frac{3}{10} - \frac{\lambda_1}{120}\right) - \delta_1^2\left(\frac{1}{15} - \frac{\lambda_1}{360}\right) - \frac{\gamma_1}{40}$$

and substitution of the above equation into (5) yields

$$\frac{U}{U_c} = 1 - \delta_1\left(\frac{3}{5} - \frac{\lambda_1}{60}\right) + \delta_1^2\left(\frac{2}{15} - \frac{\lambda_1}{180}\right) + \frac{\gamma_1}{20} \quad (8)$$

describing the ratio of the instantaneous cross-sectional mean and centreline velocities.

If $\bar{U}_c$ is defined as

$$\bar{U}_c = \frac{U_c}{U}$$

the implementation of equation (5) in differentiated form, together with the definitions of λ_1 and γ_1, into equation (3) leads to

$$\frac{1}{\bar{U}_c}\frac{d\bar{U}_c}{dt} + \frac{1}{U}\frac{dU}{dt}\left(1 - \frac{1}{\bar{U}_c}\right) = 2\left[2\delta_1 - \delta_1^2(6 + \delta_1)\gamma_1 + \frac{1}{\delta_1}\left(2 + \frac{\lambda_1}{6} - \gamma_1\right)\right] \quad (9)$$

which may be solved in conjunction with equation (8) and the definition for λ_1 which follows:

$$\lambda_1 = \frac{6(\lambda - 2\delta_1)}{6 + \delta_1} = 6\left(\frac{\delta_1^2}{\bar{U}_c}\frac{d\bar{U}_c}{dt} - 2\delta_1\right)/(6 + \delta_1) \quad (10)$$

It is appropriate to consider the initial and final zones separately. It may be recalled that these refer to the periods of time before and after the merging of the boundary layers, respectively.

3.3 Initial zone equations

As a consequence of the fact that $\gamma_1 = 0$ in this zone, the governing equations are

$$\frac{d\bar{U}_c}{dt} = \mathscr{F}_1(\alpha, \delta_1)\bar{U}_c + \mathscr{F}_2(\alpha, \delta_1) \quad (11)$$

$$\frac{1}{\bar{U}_c} = \lambda_1\mathscr{F}_3(\delta_1) + \mathscr{F}_4(\delta_1) \quad (12)$$

$$\lambda_1 = \mathscr{F}_5(\lambda, \delta_1) \quad (13)$$

where α is an 'acceleration' parameter given by

$$\alpha = \frac{1}{U}\frac{dU}{dt}$$

and $\mathscr{F}_1$, $\mathscr{F}_2$, $\mathscr{F}_3$, $\mathscr{F}_4$ and $\mathscr{F}_5$ are defined in appendix A.

Equations (11), (12) and (13) are a coupled set which may be solved for any specified variation of α with time.

3.4 Final zone equations

In this zone, $\delta_1 = 1$ and equations (8), (9), (10) may be combined to give

$$\frac{d\bar{U}_c}{dt} = \zeta_1(\alpha)\bar{U}_c + \zeta_2(\alpha) \quad (14)$$

where

$$\zeta_1(\alpha) = \frac{\alpha}{3} + 40$$

$$\zeta_2(\alpha) = \frac{\alpha}{3} + 80$$

3.5 The velocity profile shape parameter

A convenient dimensionless group which characterizes the shear stress variation in unsteady duct flow systems, is

$$S = \frac{\tau_w d}{\mu U} \quad (15)$$

where U is the cross-sectional mean velocity, and τ_w is the wall shear stress.

The parameter S may be interpreted as one whose value reflects the shape of the velocity profile. For exam-

ple, $S = 8$ corresponds to steady state Hagen-Poiseuille flow, while $S > 8$ and $S < 8$ refer to accelerating and decelerating flows, respectively.

It was appropriate to evaluate the parameter analytically, in order to serve as a comparison between different analyses, as well as enabling subsequent experimental verification of the theory.

Thus, equation (7) may be differentiated to yield τ_w, which leads to

$$S = \frac{2}{\delta_1}\bar{U}_c\left(2 + \frac{\lambda_1}{6} - \gamma_1\right)$$

3.6 Limiting values of the parameters

For the purpose of verifying the computation, as well as understanding the flow mechanisms, it is worthwhile to examine the limiting values that the parameters approach in each of the various regimes.

The acceleration parameter α is of central importance in characterizing the regimes. It may be loosely interpreted as the ratio of the gross inertia forces to the viscous forces acting in the system. It must be understood, however, that when α is zero, detailed inertia effects are not necessarily absent – the flow may still be developmental.

(*a*) *Initial zone.* This zone is finite for $\alpha \leq 7.059$ and extends indefinitely for $\alpha > 7.059$. Hence, each range is considered independently.

If $\alpha \leq 7.059$ the end of the initial zone is defined by $\delta_1 = 1$. Hence equations (12) and (13) lead to

$$\lambda_1 = \frac{42\alpha - 180}{\alpha - 75}$$

$$\bar{U}_c = \frac{\alpha - 75}{\alpha - 42}$$

$$S = 18\frac{\alpha - 20}{\alpha - 42}$$

Thus, the velocity profile shape parameter, S has the value 8.57 at the end of the initial zone for $\alpha = 0$ – an impulsively started flow.

If $\alpha > 7.059$ the boundary layers do not merge and the final zone never occurs. Hence, the values at the end of the initial zone define the values finally reached, with $\delta_1 < 1$ and $d\bar{U}_c/d\bar{t} = 0$.

Accordingly, equations (11), (12) and (13) were used to obtain the value in Table 1.

(*b*) *Final zone.* This zone exists only for $\alpha < 7.059$. Here, the limiting values are defined by $\delta_1 = 1$ and

$$\frac{d\bar{U}_c}{dt} = 0$$

which, when implemented in equation (14), lead to

$$\lambda_1 = -\frac{12}{7}$$

$$\bar{U}_c = \frac{\alpha + 240}{\alpha + 120}$$

$$\gamma_1 = \frac{4}{21}\frac{51\alpha - 360}{\alpha + 240}$$

$$S = 8\frac{120 - 2\alpha}{\alpha + 120}$$

Figures 2 to 5 show the values which δ_1, $\bar{U}_c$ and S achieve in the areas of interest.

3.7 Solution of the governing equations

(*a*) *Impulsively started flow.* A limiting case which is of interest, is the velocity profile development which occurs subsequent to a step increase of flow from rest. This hypothetical limit, which may be only approximated in practice, is consistent with $\alpha = 0$ for all $\bar{t}$, except $\bar{t} = 0$, at which time it is infinite.

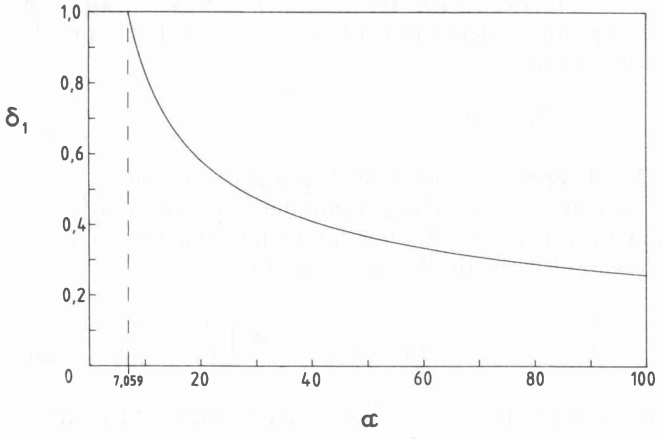

Figure 2 – Maximum values attained by the dimensionless boundary layer thickness for varying acceleration parameter

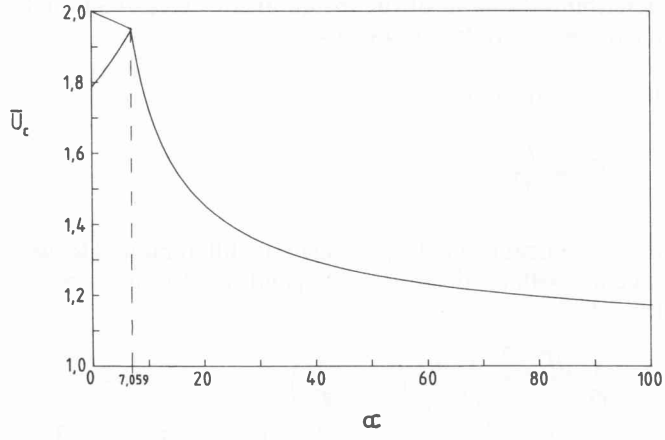

Figure 3 – Maximum values attained by the dimensionless centreline velocity for varying acceleration parameter

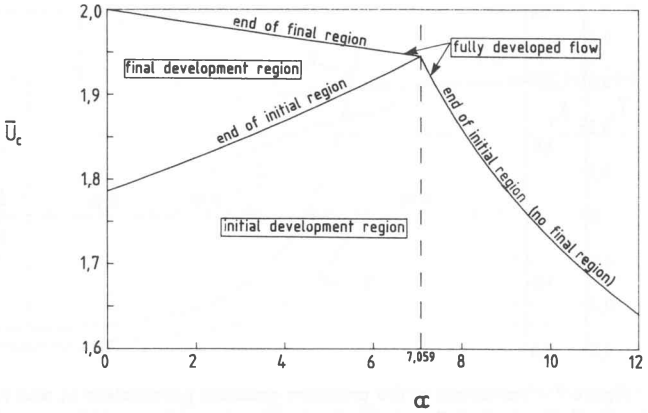

Figure 4 – Maximum values attained by the dimensionless centreline velocity for varying acceleration parameter, emphasizing the detail of the 'triple point'

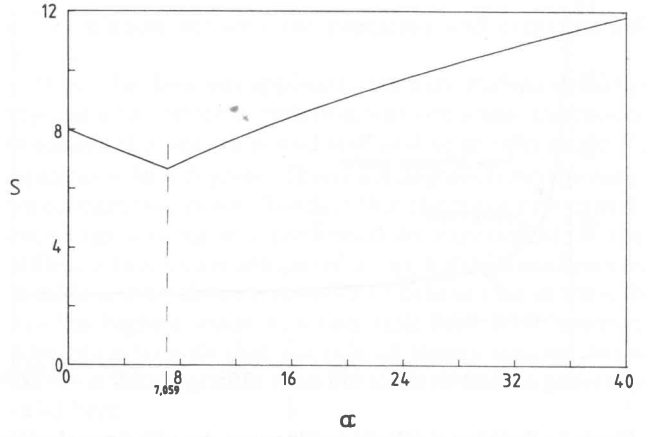

Figure 5 – Final values of velocity profile parameter for varying acceleration parameter

In this instance, equations (11), (12) and (13) of the initial zone become

$$\frac{d\bar{U}_c}{dt} = \mathscr{H}_1(\delta_1)\bar{U}_c$$

$$\frac{1}{\bar{U}_c} = \lambda_1\mathscr{H}_2(\delta_1) + \mathscr{H}_3(\delta_1)$$

$$\lambda_1 = \mathscr{H}_4(\delta_1)$$

where $\mathscr{H}_1$, $\mathscr{H}_2$, $\mathscr{H}_3$ and $\mathscr{H}_4$ are defined in Appendix A.

These may be combined to give the implicit expression for δ_1 below.

$$\bar{t} = \int_0^{\delta_1} \frac{v}{24}\,\frac{108 - 96v + 26v^2 - 2v^3}{30 - 23v + 8v^2 - v^3}dv$$

with $\bar{U}_c = 25/14$ at the time corresponding to which the boundary layers merge ($\delta_1 = 1$).

Equation (14) of the final zone becomes

$$\frac{d\bar{U}_c}{dt} = 40(2 - \bar{U}_c)$$

together with

$$\lambda_1 = \frac{480}{7}\left(\frac{1}{\bar{U}_c} - \frac{14}{25}\right) + \frac{12}{5}$$

$$\gamma_1 = \frac{100}{21}\left(\frac{1}{\bar{U}_c} - \frac{14}{25}\right)$$

The above equation has the solution

$$\bar{U}_c = 2 - \frac{1}{40}e^{-40(\bar{t} + \mathscr{A})}$$

where $\mathscr{A}$ is a constant of integration, to be satisfied by the boundary condition

$$\bar{U}_c = \frac{25}{14} \text{ at } \bar{t} = \int_0^1 \frac{v}{24}\,\frac{108 - 96v + 26v^2 - 2v^3}{30 - 23v + 8v^2 - v^3}dv.$$

The above equations were solved using a microcomputer. Figures 6 to 9 show plots of δ_1, λ_1, γ_1, $\bar{U}_c$ and S for an impulsively started flow. Figure 9 provides a comparison between the present analysis, results yielded by the analysis of Zielke [4], and those from a finite difference computer programme.

(*b*) *Exponential increase of flow rate.* when α is a non-zero, implying the existence of a time-varying cross-sectional mean velocity $U(t)$, equations (11), (12) and (13) must be solved in the initial zone and (14) in the final zone. For the purpose of this exercise, constant values of α were chosen, consistent with an exponential variation of cross-sectional mean velocity.

The solution procedure in the initial zone relies on the fact that, for constant α, the functions $\mathscr{F}_1$, and $\mathscr{F}_2$ of equation (11) become implicitly dependent on $\bar{U}_c$, via equations (12) and (13).

Implementation of constant α (> 7.059) in the final zone leads to the analytic solution

$$\bar{U}_c = \frac{1}{\zeta_1(\alpha)}\left(e^{\zeta_1(\alpha)\bar{t} + C} - \zeta_2(\alpha)\right)$$

where $\zeta_1(\alpha$ and $\zeta_2(\alpha)$ were defined previously and C is a constant whose value is decided by the values U_c and $\bar{t}$ at the end of the initial zone.

Figures 10 to 14 presents plots of δ_1, U_c, λ_1, γ_1 and S for various values of α.

4. Results and Evaluations

The analysis offers an increased understanding of the mechanisms which occur when fluid in a smooth pipe, isolated from end effects, is accelerated from rest. An integrated form of the laminar equations of motion was used, based on a fourth-degree polynomial velocity profile, and assuming the existence of a well-defined boundary layer which may coalesce at an intermediate stage of the development.

Figures 6 to 9 present the predictions for $\alpha = 0$, the dynamic development subsequent to a step increase of flow rate. An initial zone with a potential core may be identified, followed by a final zone in which the velocity

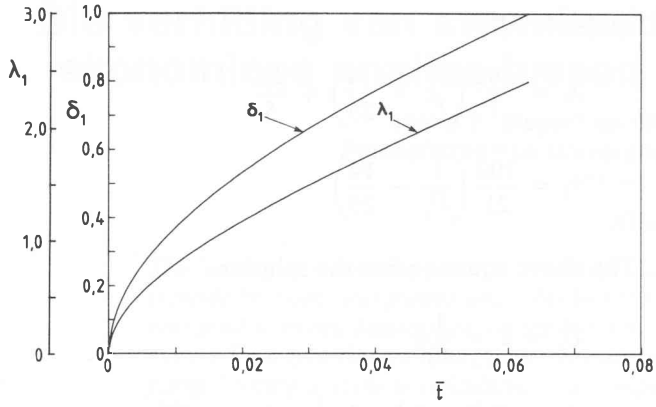

Figure 6 – Variations of dimensionless boundary layer thickness δ_1 and pressure gradient parameter λ_1 with dimensionless time in the initial region for an impulsively started flow ($\alpha = 0$)

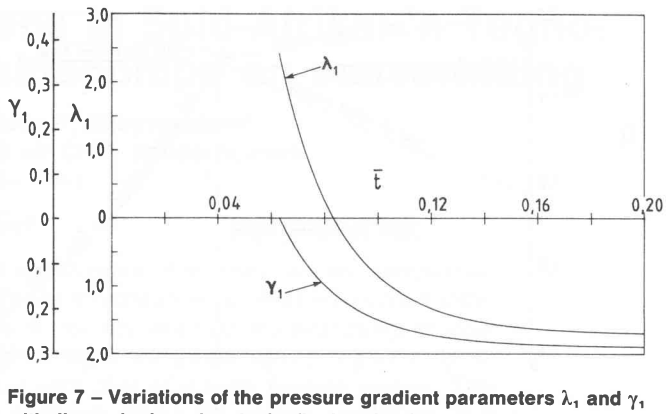

Figure 7 – Variations of the pressure gradient parameters λ_1 and γ_1 with dimensionless time in the final region for an impulsively started flow ($\alpha = 0$)

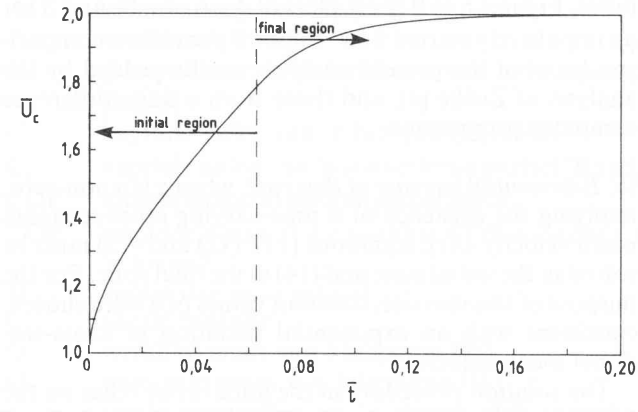

Figure 8 – Variation of dimensionless centreline with dimensionless time in the initial and final regions for an impulsively started flow ($\alpha = 0$)

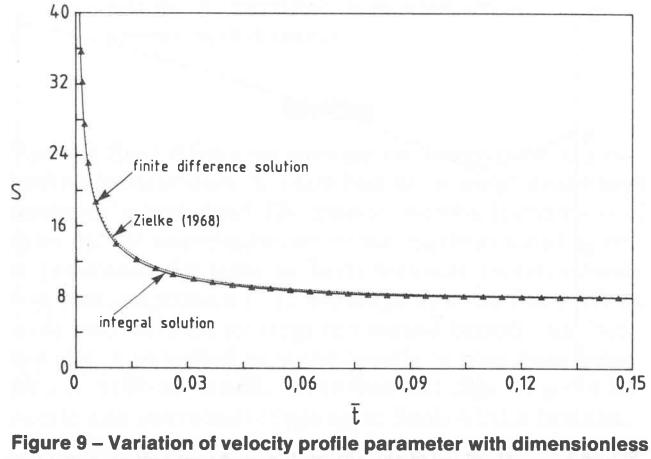

Figure 9 – Variation of velocity profile parameter with dimensionless time for an impulsively started flow, showing a comparison between the present finite difference and integral solutions, and results based on Zielke's (1968) solution

profile, consisting of merged boundary layers, approaches a parabolic shape. This essentially parallels the results of Mohanty and Asthana [5], who used a similar method in order to study the spatial laminar flow development in the entrance region of a smooth pipe.

The solution shows that the rate of change of δ_1 with time is non-zero when the boundary layers merge (according to figure 6, at approximately $\bar{t} = 0.063$). In the subsequent zone, $\lambda_1, \gamma_1, \bar{U}_c$ and S tend towards asymptotic values of $-12/7$, $-2/7$, 2 and 8, respectively (figures 7 to 9). These values are achieved at about $\bar{t} = 0.2$. Thus, despite the fact that the major change in S (between ∞ and 8.57) occurs during the initial development period, this is less than 1/3 of the total development time.

The variation of velocity profile parameter with dimensionless time yielded by the integral analysis for an impulsively started flow is shown in figure 9, together with, for the purposes of comparison, results yielded both by the analysis of Zielke [4] and by a finite difference approach of the present author. The three approaches deviated from each other by a maximum of about three percent throughout the range.

It is important to note the manner in which the present work clarifies the occurrence of certain flow regimes:

As in the spatial development case (similar to the limit $\alpha = 0$ in this analysis), distinct zones prior to and after the merging of the boundary layers are apparent for small values of α. However, as α is increased beyond a critical value of 7.059, an indefinite core region occurs adjacent to which the boundary layers never merge.

Figures 2 to 5 illustrate the manner in which the final values of δ_1, $\bar{U}_c$ and S are affected by α. For $\alpha \leq 7.059$, the final values are achieved at the end of the final zone, while for $\alpha > 7.059$, at the end of the initial zone.

Figures 3 and 4 are particularly informative, in that they emphasize the fact that as α is increased from zero, the range of $\bar{U}_c$'s between the end of the initial and final zones reduces progressively. When $\alpha = 7.059$ is reached, a 'triple' point is defined, beyond which only a single (initial) zone exists.

Figure 5 shows that S may fall below the value 8 for accelerating flows, achieving a minimum value of 6.667 for $\alpha = 7.059$. This intuitively unexpected result implies the possible occurrence of velocity profiles more triangu-

lated, or inflexional, than in the parabolic case. The explanation for this phenomenon is clear from figures 12 and 13, and the definition for S, reiterated below:

$$S = \frac{2}{\delta_1}\bar{U}_c\left(2 + \frac{\lambda_1}{6} - \gamma_1\right)$$

The minimum value of λ_1, attained for all values of $\alpha \leq 7.059$, is $-12/7$. Additionally, γ_1 varies between 0 at $\alpha = 7.059$ and $-2/7$ at $\alpha = 0$, while δ_1 achieves its maximum value of unity for the range $7.059 > \alpha > 0$. The combination of these factors, together with the fact that, within the above range, the dimensionless centreline $\bar{U}_c$ achieves a minimum value of 1.944, results in values of S less than eight.

Although the above explanation elucidates the mathematical reasons for the above-mentioned result, its physical significance requires clarification via further analysis and experimentation.

A clear shortcoming of the method is the manner in which it leads to singularities for certain of the parameters at the interface between the initial and final zones (for example, see figures 10, 12 and 13). The correlation between this solution and others for an impulsively started flow (figure 9) suggests that anomalies (only present for $\alpha < 7.059$), are confined to an insignificant time interval, however.

The favourable comparison with the computer solution for $\alpha = 0$ adds general credibility to the approach. On the basis of the fact that the singularities were equally in evidence for this limiting case as for values of α exceeding zero, it is cautiously expected that the validity of the method would extend to the whole range of α's. However, this remains to be confirmed.

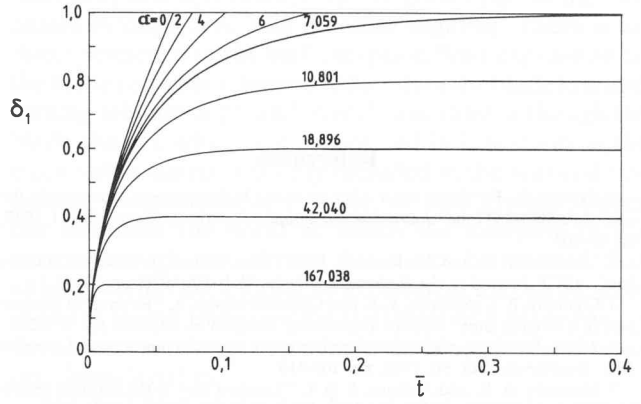

Figure 10 – Variations of dimensionless boundary layer thickness with dimensionless time for different values of the acceleration parameter

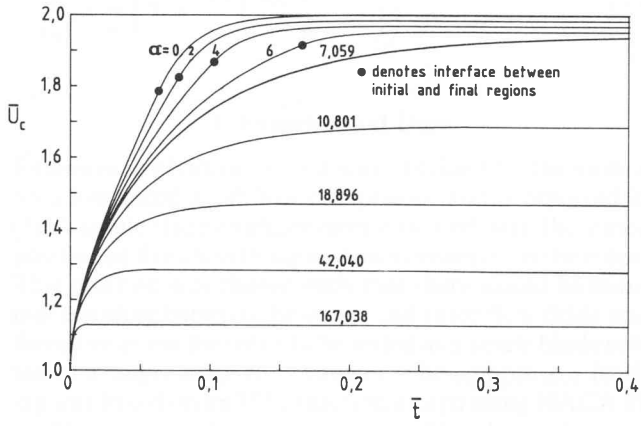

Figure 11 – Variations of dimensionless centreline velocity with dimensionless time for different values of the acceleration parameter

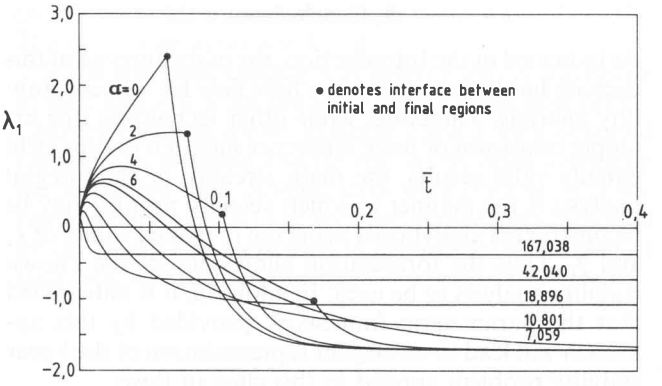

Figure 12 – Variations of the pressure gradient parameter λ_1 with dimensionless time for different values of the acceleration parameter

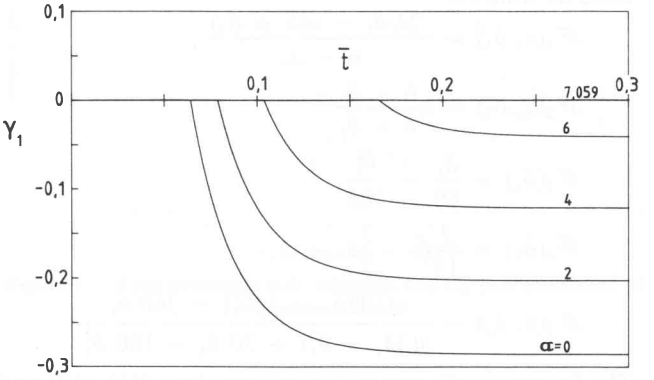

Figure 13 – Variations of the pressure gradient parameter γ_1 with dimensionless time for different values of the acceleration parameter

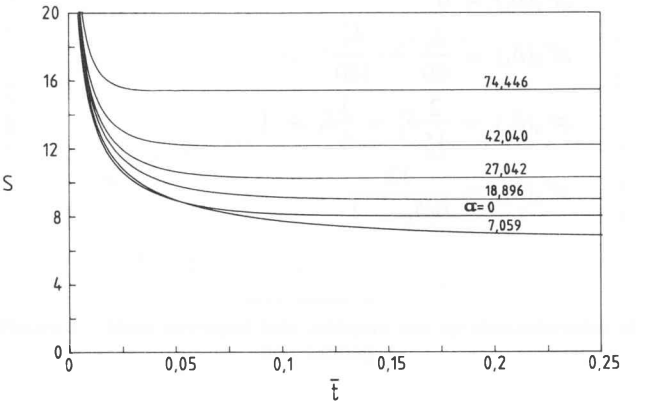

Figure 14 – Variations of velocity profile parameter with dimensionless time for different values of the acceleration parameter

5. Conclusion

As indicated in the Introduction, the main purpose of this exercise has been to provide a base flow for a linear stability analysis. Therefore, while other techniques (for example transform or finite difference methods) might yield equally valid results, the main strength of the integral analysis is the manner in which velocity profiles may be reconstructed analytically using the predicted values of λ_1 and γ_1. Thus the formulation allows any of the known stability analysis to be used. In addition, it is anticipated that the parameteric framework provided by this approach will lead to an elegant representation of the linear stability problem applied to this class of flows.

Appendix A

The functions $\mathscr{F}_i$ in equaitons (11), (12) and (13) are defined as follows:

$$\mathscr{F}_1(\alpha, \delta_1) = \frac{24/\delta_1 - \alpha(6 + \delta_1)}{6 - \delta_1}$$

$$\mathscr{F}_2(\alpha, \delta_1) = \alpha\frac{6 + \delta_1}{6 - \delta_1}$$

$$\mathscr{F}_3(\delta_1) = \frac{\delta_1}{60} - \frac{\delta_1^2}{180}$$

$$\mathscr{F}_4(\delta_1) = \frac{2}{15}\delta_1^2 - \frac{3}{5}\delta_1 + 1$$

$$\mathscr{F}_5(\alpha, \delta_1) = \frac{\alpha(108\delta_1 - 24\delta_1^2) - 360/\delta_1}{\alpha(3\delta_1 - \delta_1^2) + 30/\delta_1 - 180/\delta_1^2}$$

The functions $\mathscr{H}_i$ pertaining to equations (11), (12) and (13) when $\alpha = 0$ are

$$\mathscr{H}_1(\delta_1) = \frac{24}{\delta_1(6 - \delta_1)}$$

$$\mathscr{H}_2(\delta_1) = 0$$

$$\mathscr{H}_3(\delta_1) = \frac{\delta_1}{60} - \frac{\delta_1^2}{180}$$

$$\mathscr{H}_4(\delta_1) = \frac{2}{15}\delta_1^2 - \frac{3}{5}\delta_1 + 1$$

$$\mathscr{H}_5(\delta_1) = \frac{12}{6/\delta_1 - 1}$$

Table 1 Asymptotic values of the parameters in the initial region for $\alpha > 7.059$

δ_1	α	λ_1	$\tilde{U}_c$	S
0.1	667.037	0.197	1.063	41.810
0.2	167.038	0.387	1.131	21.891
0.3	74.446	0.571	1.206	15.310
0.4	42.040	0.750	1.287	12.066
0.5	27.042	0.923	1.376	10.159
0.6	18.896	1.091	1.472	8.922
0.7	13.986	1.254	1.577	8.070
0.8	10.801	1.412	1.691	7.450
0.9	8.618	1.565	1.813	7.007
1.0	7.059	1.714	1.944	6.667

References

1. Szymanski, P. "Some exact solution of the hydrodynamic equations in the case of a cylindrical tube" *Journal de Mathetiques Pures et Appliques* Vol. 11, 1932, pp. 67-107.
2. Letelier, M. F. and Leutheusser, H. J. "Skin friction in unsteady laminar flow" *ASCE Journal of the Hydraulics Division* Vol 102, 1976, pp. 41-56.
3. Chambre, P. L.; Schrock, V. E. and Gopalakrishnan, A. "Reversal of laminar pipe in a circular pipe" *Nuclear Engineering Design* Vol. 47, 1978 pp. 239-250.
4. Zielke, W. "Frequency-dependent friction in transient pipe flows" *Journal of Basic Engineering* Vol. 90, 1968, pp. 109-115.
5. Mohanty, A. K. and Asthana, S. B. L. "Laminar flow in the entrance region of a smooth pipe" *Journal of Fluid Mechanics* Vol. 90, 1978, pp. 433-447.
6. Ishizawa, S. "The axisymmetric flow in an arbitrarily shaped narrow gap" *Japanese Society of Mechanical Engineers Bulletin* Vol. 9, 1966, pp. 86-103.